Correspondence

Apodization and Windowing Eigenfunctions

Kevin J. Parker, *Fellow, IEEE*

***Abstract*—Across a range of spectral estimation problems and beam focusing problems, it is necessary to constrain the properties of a function and its Fourier transform. In many cases, compact functions in both domains are desired, within the theoretical bounds of the uncertainty principle. Recently, a hyperbolic sine function of modified argument and power was found to be an approximate eigenfunction of the Fourier transform operation, and demonstrated useful properties of compactness with low side lobes. The empirical finding of the eigenfunction relationship is explained by comparison with the prolate spheroidal wave functions, which have exact eigenfunction properties, and their usefulness is demonstrated by examples.**

I. Introduction

In many applications of focused beams we apply an apodization function at the source and a focal pattern is given approximately as the Fourier transform of the apodization function. It is commonly the case that the available support for the apodization function is strictly limited, but at the same time a highly compact focal region is desired to achieve high resolution. Furthermore, in the area of spectral windowing, analogous considerations of concentrated time and frequency signals are common [1].

In considering the problem of apodization of focused ultrasound systems, and more generally the spectral windowing problem, we recently [2] introduced the useful hyperbolic sine function mapped to a limited domain:

$$F(x) = \begin{cases} (\sinh[1-x^2])^{\alpha} & -1 < x < 1 \\ 0 & \text{elsewhere.} \end{cases} \tag{1}$$

For the particular case $\alpha = 5$, this function was shown to be an approximate eigenfunction of the Fourier transform (FT) operation, meaning that its FT was also approximately described by a $\sinh^5$ function. In theory, under the uncertainty principle [3, ch. 4], no function and its Fourier transform can both have strictly limited support, and so the transform of the $\sinh^5$ function of limited support necessarily includes side lobes, however these are at a level below −78 dB, which is sufficiently negligible for many applications.

This $\sinh^5$ approximate eigenfunction pair was shown to have useful properties in the context of designing focused beam patterns, because the $\sinh^5$ apodization function and its Fourier transform (which approximates the shape of the transverse focal beam pattern [4], [5]), are both compact or localized and have a nearly parabolic fall-off of amplitude on a log or decibel scale. In this correspondence, we examine the theoretical basis for the apparent eigenfunction relation. The key concept is that the $\sinh^5$ function closely resembles a prolate spheroidal wave function (PSWF), which has a unique and useful eigenfunction relation with respect to the Fourier transform operation.

Manuscript received December 5, 2013; accepted June 4, 2014.

K. J. Parker is with the Department of Electrical and Computer Engineering, University of Rochester, Rochester, NY (e-mail: kevin.parker@rochester.edu).

DOI http://dx.doi.org/10.1109/TUFFC.2014.3071

II. Relation of $\sinh^{\alpha}$ to PSWFs

The similar functions $(\sinh[1-x^2])^5$ and the spheroidal function $\mathrm{PS}_{0,0}[14, x]$ are given in Fig. 1 (the notation and use of the PSWF will be explained in the following section). Their differences are barely distinguishable on this linear scale, and the maximum difference is on the order of 0.005, peaking between $|x| = 0.6$ and 0.7. The Fourier transforms of these two functions are given in Fig. 2, but on a decibel scale to emphasize the existence of side lobes which are important in applications that cover very wide dynamic range of signals. The two signals' transforms have a nearly identical main lobe but the lowest values, below −100 dB, correspond to the transform of the spheroidal function. Along with the lower side lobes, the spheroidal function has an exact and very useful eigenfunction property that is compatible with the requirement for limiting the domain of the aperture or window function.

III. Properties of the Prolate Spheroidal Wave Function

The central importance of the PSWFs to the problem of signals that are concentrated in both time and frequency was developed by Slepian and his colleagues at Bell Labs from 1960 onward, spurred on by a theoretical question of limits posed by Shannon [6]–[11]. There are many useful and fortunate properties of the PSWFs—so many that Slepian said "The mystery of this serendipity grows. Most of us feel that there is something deeper here than we currently understand" [11]. A full review of the PSWFs functions and their properties are well beyond the scope of this communication. However, a brief outline of the relevant properties will be given as background.

Using the notation of Slepian [6] and Moore and Cada [12], the PSWFs $\psi_n(c,t)$ concentrated in the interval of $[-t_0, t_0]$ are normalized eigenfunctions of the system

$$\int_{-t_0}^{t_0} \psi_n(c,t) \frac{\sin \Omega(x-t)}{\pi(x-t)} \,\mathrm{d}t = \psi_n(c,x)\lambda_n(c), \tag{2}$$

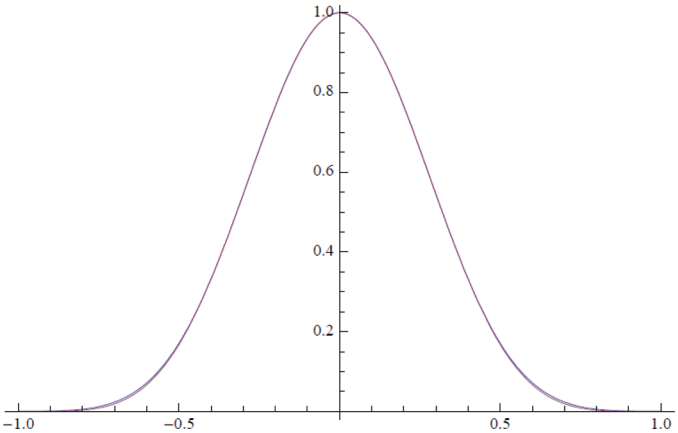

Fig. 1. Two functions (normalized to 1) are plotted over the domain $-1 < x < 1$. The functions are $(\sinh[1-x^2])^5$ and SpheroidalPS$[0,0,14,x]$. The differences are smaller than 0.005 at any point within the domain; this slight difference is most visible around $|x| = 0.7$. The $(\sinh)^5$ function is the lower of the two in this subrange.

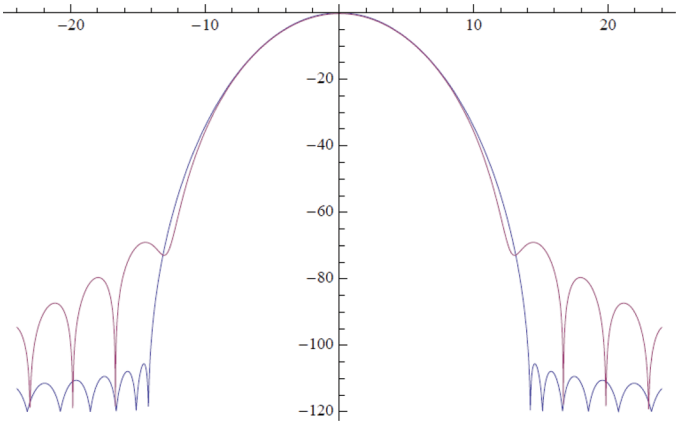

Fig. 2. The magnitude of the Fourier transform of the $\sinh^5$ and PS functions, shown on a decibel scale. The horizontal axis is spatial frequency. The PS function side lobes are below −100 dB.

where Ω is the cut-off bandwidth of the eigenfunction and $c = t_0\Omega$, a time–bandwidth product. The $\lambda_n(c)$ are the eigenvalues of the sinc kernel and can be also regarded as the index of concentration on the interval $[-t_0, t_0]$. For the sake of simplicity, we set the concentration interval to $[-1,1]$ in our implementation. Slepian [6] would sometimes suppress the parameter c, writing $\psi_n(c,t)$ as simply $\psi_n(t)$. Some of the important properties of these functions are [11]

$$\begin{aligned} &\lambda_0 > \lambda_1 > \lambda_2 > \cdots, \\ &\psi_n(x) \text{ is even or odd with } n, \\ &\psi_n(x) \text{ has exactly } n \text{ zeros in } (-1,1), \\ &\psi_n(x) \sim k_n \frac{\sin cx}{x}, \text{ as } x \to \infty, \end{aligned} \tag{3}$$

$$\int_{-1}^{1} e^{2\pi i x t} \psi_n(t) \mathrm{d}t = \alpha_n \psi_n(2\pi x/c), \quad -\infty < x < \infty, \tag{4}$$

where k_n and α_n are independent of x. Eq. (4) demonstrates an unusual and important property: the Fourier transform of $\psi_n(t)$ restricted to $|t| < 1$ has the same form as ψ_n except for a scale change. The equation can also be written

$$\psi_n(x) = \frac{1}{\alpha_n} \int_{-c/2\pi}^{c/2\pi} e^{2\pi i x t} \psi_n(2\pi t/c) \mathrm{d}t, \tag{5}$$

which shows $\psi_n(x)$ to be band-limited to bandwidth $c/2\pi$. The $\psi_n(x)$ are complete in $-\infty < x < \infty$ in the L^2 sense among signals of bandwidth $c/2\pi$ or less, i.e., complete in $B_{c/2\pi}$. Finally, the $\psi_0(c,t)$ are the most concentrated signal possible within the time and band limits [11].

A key point useful for the application to apodization and focused beams is that a PSWF of unlimited support or extent can be concentrated (that is, have most of its energy) within the limits ± 1. If this function is strictly windowed to $|\arg| \leq 1$, its Fourier transform, properly scaled, is the original prolate spheroidal (PS) function of unlimited extent, and similarly concentrated near the origin. It is worth noting that for other general functions, such as the Gaussian, the Fourier transform of the function after strict truncation [as implied by the limits of integration of (4) or (5)] will be the Fourier transform of the original function convolved with a sinc function [3, ch. 2]. This typically creates extensive side lobes, as demonstrated in [2] and as will be shown later in Fig. 5(a). The PSWFs also have side lobes, but retain the maximum concentration within the main lobe. For some applications of ultrasound imaging, we therefore seek PSWFs that are concentrated near the origin and that have very low (less than −70 dB relative amplitude for typical ultrasound applications) side lobes outside the limits of $|\arg| \leq 1$.

To do this, an additional comment on notation in necessary. The generalized angular spheroidal wave function $S_{n,m}(c,x)$ discussed in [13] and [14] has a direct relation to Slepian's functions. We use the Mathematica (Wolfram Research, Champaign, IL) function SpheroidalPS$[n,0,c,x]$, alternatively denoted as $\mathrm{PS}_{n,0}[c,x]$, as the equivalent to $\psi_n(c,x)$ as given in (2).

Using the property that the nth eigenmode has exactly n zeros within the range $[-1,1]$, and now applying this to the problem of a compact and positive main lobe, we examine the particular case of $n = 0$.

Fig. 3(a) shows the PSWF $[0,0,c,x]$ for three cases: $c = 9$ (widest curve), $c = 12$, and $c = 15$ (narrowest curve). The c parameter is related to the limits of the bandwidth of the signal. The case $c = 15$ has the largest bandwidth and also has the narrowest lobe. Fig. 3(b) shows the signals outside of the domain $|x| < 1$. These bandlimited signals oscillate; the largest oscillations are for the case $c = 9$ and smaller values are found for $c = 12$. The signal for $c = 15$ is too small to be seen on this scale. For comparison, the $\sinh^\alpha$ functions are given in Fig. 4 for the cases $\alpha =$

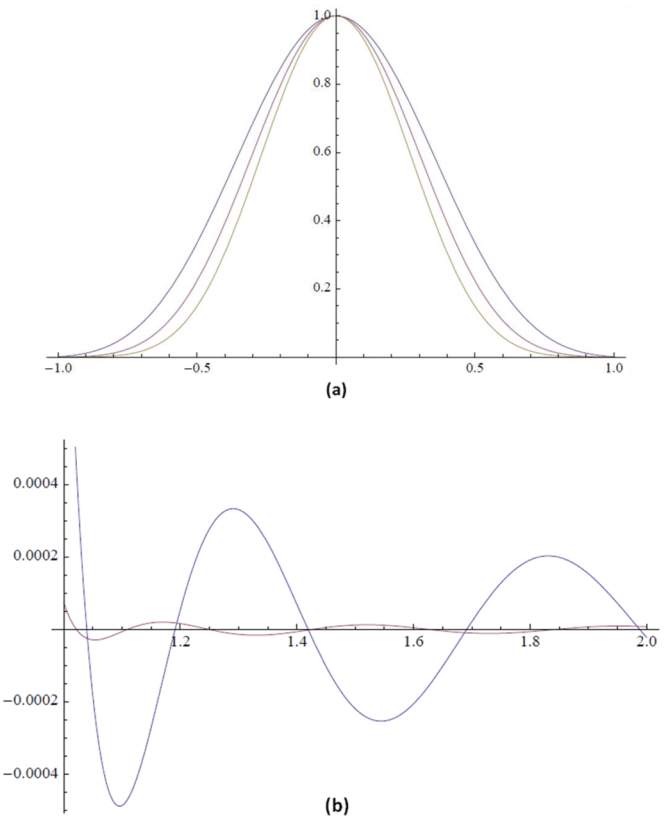

Fig. 3. (a) The PSWF behavior as a function of the bandwidth parameter c. Shown are normalized values over the domain $-1 < x < 1$ for SpheroidalPS$[0, 0, c, x]$, where $c = 9$ (widest function), $c = 12$, and $c = 15$ (narrowest function). (b) The PSWF behavior outside of the domain $|x| < 1$, as a function of the bandwidth parameter c. The largest oscillation corresponds to $c = 9$ (the narrowest band); the smaller function corresponds to $c = 12$.

3 (widest curve), $\alpha = 4$, and $\alpha = 5.5$ (narrowest curve). These functions have similar characteristics to the PSWF within the domain of $|x| < 1$, and are defined to be zero outside of the region of support.

IV. Results

A comparison of apodization functions and their transforms are given in Table I. The energy term is the integral of the square of the normalized function over the range of apodization, -1 to $+1$. The Rect function is simply the entire apodization at maximum transmit (or receive)

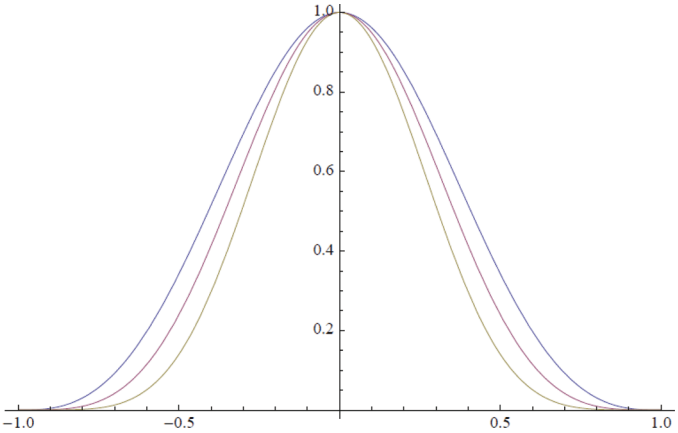

Fig. 4. The functions $(\sinh[1 - x^2])^\alpha$ are shown for $\alpha = 3$ (widest curve), $\alpha = 4$, and $\alpha = 5.5$ (narrowest curve). These are approximations to the PS functions shown in Fig. 3(a).

gain, and so represents 100%. The Rect function has the highest side lobe levels, however, and therefore more suitable functions are typically used, but with the tradeoff of lowered energy. The Gaussian function is truncated at 5σ over the standard interval of $-1 \le x \le 1$, so $\sigma = 0.4$. The widely used Blackman window is defined by $0.42 + 0.5\cos[\pi x] + 0.08\cos[2\pi x]$ over the standard interval. The PSWFs become progressively narrower as the bandwidth parameter increases from 9 to 15. At the same time, the -6-dB beamwidth of the transform increases slightly, while the maximum side lobe levels drop significantly. The $\sinh^\alpha$ functions are listed as approximate functions for reference, but are rounded values for simplicity. A least-squares error best fit would provide more precise values of α. In practice, the $\sinh^\alpha$ functions are easier to compute and manipulate than the PS functions. However, the $\sinh^\alpha$ functions have significantly (over 10 dB) higher side lobe levels compared with the PSWFs.

V. Discussion

One way to evaluate the combination of factors is to examine the image produced from a pair of reflectors separated by a small distance. Fig. 5(a) shows the image of two point reflectors separated by 4.68 mm laterally, at the focus of a 5-MHz, f-number 3.2 simulated imaging system using the Field II acoustic pressure field simulation pack-

TABLE I. Comparison of Apodization Functions.

	Energy % of maximum	-6-dB beamwidth (normalized units)	Side lobe maximum level (dB)	Approximate function
Rect	100	3.8	-13	·
Gauss 5σ	35	6.0	-43	·
Blackman	30	7.2	-57	·
$PS_{0,0}(9, x)$	30	7.0	-65	$\sinh[\cdot]^3$
$PS_{0,0}(12, x)$	26	8.2	-92	$\sinh[\cdot]^4$
$PS_{0,0}(14, x)$	24	8.8	-107	$\sinh[\cdot]^5$

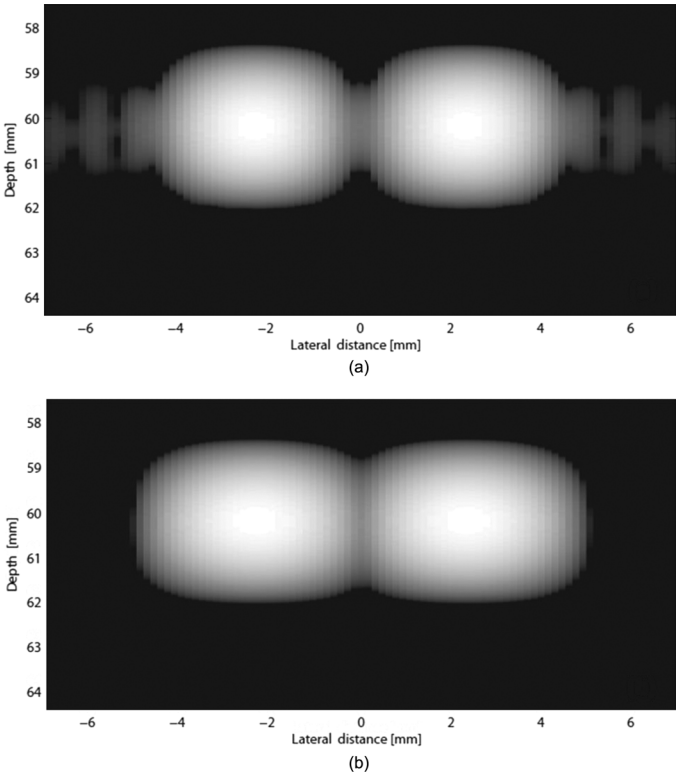

Fig. 5. Simulated images from a 5-MHz, f-number 3.2 simulated scanner using Field II and a pair of scatterers at the focus, 60 mm depth and 4.68 mm separation laterally. In the simulation, the transducer had 129 active elements, a narrowband pulse (−6-dB bandwidth of 20%) was transmitted, and the apodization function was used on both transmit and receive. Images are 100 dB dynamic range scale so that one-way side lobes down to −50 dB can be visualized. (a) A Gaussian 5σ truncated apodization is employed. Side lobes are a result of truncation. (b) The SpheroidalPS$[0, 0, 9, x]$ function is used for apodization. No side lobes are visible within −100 dB dynamic range.

age [15]. A 100 dB dynamic range gray scale is used to visualize side lobes that would be above −50 dB one-way. A 5σ truncated Gaussian apodization is used in Fig. 5(a) in both transmit and receive modes. The truncation results in low-level side lobes. The function SpheroidalPS$[0, 0, 9, x]$ was used as an apodization function in Fig. 5(b). This has a slightly larger main lobe than the truncated 5σ Gaussian but much reduced side lobes (not visible on 100 dB dynamic range gray scale). Similar images from other apodization functions can be compared in [2].

Finally, we note that a discrete version of the PSWF window has been applied to digital signal processing (DSP) applications [10], [16]. In addition, Harris [1] asserts that the discrete Fourier transform versions of the Barcilon–Temes window and the Kaisar–Bessel windows are approximations of Slepian's functions.

VI. Conclusion

Around 1960, Slepian and colleagues considered the important class of problems in communications theory concerning signals that are concentrated in time and frequency. Within the general time–frequency uncertainty principal, no signal can be both time-limited and band-limited, so the important practical question pertains to how we can maximize the concentration of signals in both domains. Out of this came a set of remarkable papers and developments that pertain to the PSWFs [6]–[11]. The apodization of focused beams is a closely related problem, as designers seek to concentrate the apodization function across a strictly limited aperture, while simultaneously concentrating the focal beampattern that is produced (which can be approximated by the Fourier transform of the apodization function in many cases). Because of the similar considerations, the PSWFs can have an equally useful role in applications to the design of apodization and beampattern functions. Specifically, the SpheroidalPS$[0, 0, c, x]$ function is an eigenfunction of the Fourier transform operation and is maximally concentrated over $-1 < x < 1$. Simultaneously, this function is maximally concentrated in the transform domain within limits related to the parameter c. A consequence of this fortunate property is very low side lobes compared with many other common window functions. The only disadvantage of the PSWFs is their computational complexity: they exist as callable functions in Mathematica, but must be calculated from their defining expansions [14]. For simplicity, the $\sinh^{\alpha}$ functions can be used as approximations if desired.

Acknowledgments

The author is indebted to Professor A. Clark for his insights and to S. Chen for expert modeling.

References

[1] F. J. Harris, "On the use of windows for harmonic analysis with the discrete Fourier transform," *Proc. IEEE*, vol. 66, no. 1, pp. 51–83, 1978.

[2] K. J. Parker, "Apodization and windowing functions," *IEEE Trans. Ultrason. Ferroelectr. Freq. Control*, vol. 60, no. 6, pp. 1263–1271, 2013.

[3] A. Papoulis, *The Fourier Integral and its Applications (McGraw-Hill Classic Textbook Reissue Series)*, New York, NY: McGraw-Hill, 1987.

[4] A. Macovski, *Medical Imaging Systems* (Prentice-Hall information and system sciences series), Englewood Cliffs, NJ: Prentice-Hall, 1983, ch. 9.

[5] J. W. Goodman, *Introduction to Fourier Optics* (McGraw-Hill physical and quantum electronics series), Englewood, CO: Roberts & Co., 2005.

[6] D. Slepian and H. O. Pollak, "Prolate spheroidal wave functions, Fourier analysis and uncertainty. 1," *Bell Syst. Tech. J.*, vol. 40, no. 1, pp. 43–63, 1961.

[7] H. J. Landau and H. O. Pollak, "Prolate spheroidal wave functions, Fourier analysis and uncertainty. 2," *Bell Syst. Tech. J.*, vol. 40, no. 1, pp. 65–84, 1961.

[8] H. J. Landau and H. O. Pollak, "Prolate spheroidal wave functions, Fourier analysis and uncertainty. 3. Dimension of space of essentially time- and band-limited signals," *Bell Syst. Tech. J.*, vol. 41, no. 4, pp. 1295–1336, 1962.

[9] D. Slepian, "Prolate spheroidal wave functions Fourier analysis and uncertainty. 4. Extensions to many dimensions—Generalized pro-

late spheroidal functions," *Bell Syst. Tech. J.*, vol. 43, no. 6, pp. 3009–3057, 1964.
[10] D. Slepian, "Prolate spheroidal wave-functions, Fourier-analysis, and uncertainty. 5. Discrete case," *Bell Syst. Tech. J.*, vol. 57, no. 5, pp. 1371–1430, 1978.
[11] D. Slepian, "Some comments on Fourier-analysis, uncertainty and modeling," *SIAM Rev.*, vol. 25, no. 3, pp. 379–393, 1983.
[12] I. C. Moore and M. Cada, "Prolate spheroidal wave functions, an introduction to the Slepian series and its properties," *Appl. Comput. Harmon. Anal.*, vol. 16, no. 3, pp. 208–230, May 2004.
[13] C. Flammer, *Spheroidal Wave Functions*, Stanford, CA: Stanford University Press, 1957.
[14] M. Abramowitz and I. A. Stegun, *Handbook of Mathematical Functions With Formulas, Graphs, and Mathematical Tables*, Washington, DC: U.S. Government Printing Office, 1964.
[15] J. A. Jensen, "Simulation of advanced ultrasound systems using Field II," in *IEEE Int. Symp. Biomedical Imaging: Nano to Macro*, 2004. vol. 1, pp. 636–639.
[16] L. C. Barbosa, "A maximum-energy-concentration spectral window," *IBM J. Res. Develop.*, vol. 30, no. 3, pp. 321–325, May. 1986.